University of Huddersfield Repository

Liu, S, Gu, Fengshou and Ball, Andrew

The on-line detection of engine misfire at low speed using multiple feature fusion with fuzzy pattern recognition

Original Citation

Liu, S, Gu, Fengshou and Ball, Andrew (2002) The on-line detection of engine misfire at low speed using multiple feature fusion with fuzzy pattern recognition. Proceedings of the Institution of Mechanical Engineers Part D Journal of Automobile Engineering, 216 (5). pp. 391-402. ISSN 0954-4070

This version is available at https://eprints.hud.ac.uk/id/eprint/6808/

http://eprints.hud.ac.uk/

The on-line detection of engine misfire at low speed using multiple feature fusion with fuzzy pattern recognition

S Liu[1]*, **F Gu**[2] and **A Ball**[2]
[1]School of Mechanical Science and Engineering, Huazhong University of Science and Technology, Wuhan, People's Republic of China
[2]Maintenance Engineering Research Group, School of Engineering, University of Manchester, Manchester, UK

Abstract: This paper proposes a technique for the on-line detection of incipient engine misfire based on multiple feature fusion and fuzzy pattern recognition. The technique requires the measurement of instantaneous angular velocity signals. By processing the engine dynamics model equation in the angular frequency domain, four dimensionless features for misfire detection are defined, along with fast feature-extracting algorithms. By directly analysing the waveforms of the angular velocity and the angular acceleration, six other dimensionless features are extracted. Via fuzzy pattern recognition, all the features are associated together as a fuzzy vector. This vector identifies whether the engine is healthy or faulty and then locates the position of a misfiring cylinder or cylinders if necessary. The experimental work conducted on a production engine operating at low speeds confirms that such a technique is able to work with the redundant and complementary information of all the features and that it leads to improved diagnostic reliability. It is fully expected that this technique will be simple to implement and will provide a useful practical tool for the on-line monitoring and real-time diagnosis of engine misfire in individual cylinders.

NOTATION

a_m, b_m	mth element of $\boldsymbol{A}$ and $\boldsymbol{B}$
$\bar{A}^{(n)}$	estimate of angular acceleration fluctuation of nth cylinder
$\boldsymbol{A}, \boldsymbol{B}$	fuzzy vector
c_m, d_m	constant
DFT	discrete Fourier transform
$h(\theta)$	impulse response function of engine dynamics model
$H(\lambda)$	Fourier transform of $h(\theta)$
i	$= \sqrt{-1}$
$I_A^{(n)}$	acceleration variation index of nth cylinder
$I_C^{(n)}$	angular variation index of nth cylinder
$I_F^{(n)}$	acceleration fluctuation index of nth cylinder
$I_H^{(n)}$	maximum acceleration index of nth cylinder
$I_L^{(n)}$	minimum acceleration index of nth cylinder
$I_S^{(n)}$	summed acceleration index of nth cylinder
$I_T^{(n)}$	torque fluctuation index of nth cylinder
$I_V^{(n)}$	velocity variation index of nth cylinder
J	moment of inertia
K	number of frequency harmonics utilized
L	number of data samples per engine cycle
M	dimension of $\boldsymbol{A}$ and $\boldsymbol{B}$
n	cylinder number
N	number of cylinders
R_F	acceleration component ratio
R_T	torque component ratio
$R_{T,0}$	threshold for R_T
t	time
$T_e(\theta)$	rotating inertia torque
$T_e(\lambda)$	Fourier transform of $T_e(\theta)$

$T_L(\theta)$ total resistive torque

$T_L(\lambda)$ Fourier transform of $T_L(\theta)$

$T_p(m\lambda_c)$ DFT of $T_p(\theta)$ at $m\lambda_c$, for $T_p(\theta)$ within one engine cycle

$T_p^{(n)}(m\lambda_f)$ DFT of $T_p(\theta)$ at $m\lambda_f$, for $T_p(\theta)$ of nth cylinder within one engine cycle

$T_p(\theta)$ gas pressure torque

$T_p(\lambda)$ Fourier transform of $T_p(\theta)$

$\bar{T}_p^{(n)}$ estimate of gas pressure torque output of nth cylinder

$T_r(\theta)$ reciprocating inertia torque

$T_r(\lambda)$ Fourier transform of $T_r(\theta)$

u_m mth element of U

U real vector

$x(\theta)$ $= [\omega(\theta)]^2$

$X(m\lambda_c)$ DFT of $x(\theta)$ at $m\lambda_c$, for $x(\theta)$ within one engine cycle

$X^{(n)}(m\lambda_f)$ DFT of $x(\theta)$ at $m\lambda_f$, for $x(\theta)$ of nth cylinder within one engine cycle

$X(\lambda)$ Fourier transform of $x(\theta)$

$\alpha(\theta)$ crankshaft angular acceleration

$\alpha_{max}^{(n)}$ peak value of angular acceleration of nth cylinder

$\alpha_{min}^{(n)}$ valley value of angular acceleration of nth cylinder

$\alpha_{sum}^{(n)}$ summed absolute value of angular acceleration of nth cylinder

ε minor positive value quite near zero

θ crankshaft angular position

$\theta_{max}^{(n)}$ crankshaft angular position corresponding to $\omega_{max}^{(n)}$

$\theta_{min}^{(n)}$ crankshaft angular position corresponding to $\omega_{min}^{(n)}$

$\Delta\theta^{(n)}$ crankshaft angular duration corresponding to $\Delta\omega^{(n)}$

$[\Delta\theta]^{(n)}$ crankshaft angular interval corresponding to nth cylinder

λ angular frequency variable

λ_c engine cycle frequency

λ_f engine firing frequency

μ fuzzification member function

σ degree of closeness between two fuzzy vectors

σ_1 maximum–minimum degree of closeness

σ_2 Euclidean distance degree of closeness

σ_0 threshold for σ_1 (or σ_2)

$\omega(\theta)$ crankshaft angular velocity

ω_k $\omega(\theta)$ sampled at point k within one engine cycle

$\omega_k^{(n)}$ $\omega(\theta)$ sampled at point k of nth cylinder within one engine cycle

$\omega_{max}^{(n)}$ peak value of angular velocity of nth cylinder

$\omega_{min}^{(n)}$ value of angular velocity of nth cylinder

$\Delta\omega^{(n)}$ maximum angular velocity variation of nth cylinder

1 INTRODUCTION

Considerable interest has been shown in the detection of incipient engine misfire in recent years. As exhaust emission control regulations become increasingly stringent, it becomes even more likely that, if possible, misfire will be monitored continuously by the on-board diagnostic system. To avoid costly engine failures and to reduce repair time, the diagnostic system should also be capable of indicating the fault location, i.e. identifying the misfiring cylinder or cylinders in an early stage.

Misfire in internal combustion engines refers to a situation where the fuel–air mixture cannot be efficiently combusted in one or more cylinders. Although direct measurement of in-cylinder pressure of each individual cylinder may be the most precise approach for misfire detection, it is obviously impractical because it requires installing a costly pressure transducer in each cylinder. However, the instantaneous angular velocity can be obtained easily and reliably, and this kind of signal may be widely utilized for engine monitoring, diagnosis and control [1–4].

The detection of engine misfire by instantaneous angular velocity measurement can be performed in two ways. The first is based on waveform analysis, in which the instantaneous velocity waveform is analysed directly and the extracted feature used to identify whether misfire exists in the engine by simple threshold or by more complicated Bayesian decision theory [5–7]. The second is based on torque estimation, in which the instantaneous gas pressure torque (indicated torque) or individual cylinder pressure is calculated by an engine dynamics model, and from this the misfiring cylinder is identified [8–17].

At present, almost all misfire detection techniques are based only on a single feature or indicator. Each technique has its own advantages and drawbacks with the result that no single technique has proven to be completely reliable over a range of operating conditions. An important consideration is that under complex conditions (such as when misfire happens simultaneously in multiple cylinders) the information required to make reliable misfire decisions may simply not be available in a single feature. The diagnostic conclusions drawn by different single features do not always concur and sometimes directly conflict [7, 16].

In recent years, multisensor data fusion has received significant attention for automated target recognition, guidance for autonomous vehicles, remote sensing, battle-field surveillance, monitoring of manufacturing process, condition-based maintenance of complex machinery, robotics and medical applications [18–20]. Data fusion techniques combine data from different sensors with related information from an associated database to achieve improved accuracy and more specific inference than can be achieved by the use of a single sensor alone. Data fusion is attractive because any loss

of sensitivity in one sensor domain can be offset by information from other sensors, enabling, in theory, successful decision-making ability over a wider range of operating conditions.

In this paper, a technique for the on-line detection of engine misfire, which employs information from multiple features, is proposed. The remainder of the paper is organized as follows. In section 2, 10 dimensionless features for misfire detection are introduced, along with fast extraction algorithms. In section 3, the architecture for the on-line misfire detection by multiple feature fusion is presented. The multiple feature fusion procedure is described in section 4. In section 5, the technique is demonstrated on experimental data from a four-cylinder four-stroke diesel engine. This study is concluded in section 6.

2 DIMENSIONLESS FEATURES AND EXTRACTION ALGORITHMS

2.1 Engine dynamics model and gas pressure torque estimation

If it is assumed that the engine is operating in a steady state condition and the crankshaft system is rigid, the non-linear engine dynamics model is based on the familiar torque balance equation [**12**–**16**]

$$J\ddot{\theta} = T_e(\theta) = T_p(\theta) - T_r(\theta) - T_L(\theta) \qquad (1)$$

where J is the effective moment of inertia of the rotating parts of the engine, θ represents the crankshaft angular position and is hence a function of time t, i.e. $\theta = \theta(t)$, $\dot{\theta} = d\theta/dt$, $\ddot{\theta} = d^2\theta/dt^2$, $T_e(\theta)$ and $T_r(\theta)$ are the rotating inertia torque (or net torque) and the reciprocating inertia torque associated with the inertia of rotating and reciprocating components respectively, $T_p(\theta)$ is the gas pressure torque (or indicated torque) due to the force generated by the combustion pressure and $T_L(\theta)$ is the total resistive torque of the engine.

Equation (1) can be further derived to a second-order non-linear differential equation [**14**], which reveals explicitly the relationship between the cylinder pressure and the instantaneous crankshaft angular velocity $\omega(\theta) = \dot{\theta}$, and thus it is possible in theory to estimate the cylinder pressure or gas pressure torque from measurements of $\omega(\theta)$. In practice, however, it is quite difficult to solve such a complex equation directly in the time domain. As shown in equation (1), the engine can be treated as a dynamic system, of which the input is the rotating inertia torque $T_e(\theta)$ and the output is the angular acceleration $\alpha(\theta) = \ddot{\theta}$. For a more general situation, supposing $h(\theta)$ to be the impulse response function of the dynamic system, its output $\alpha(\theta)$ will be given in convolution form $\alpha(\theta) = T_e(\theta) * h(\theta)$. Therefore, the estimation of the gas pressure torque (or, furthermore, the cylinder pressure) from the instantaneous angular

acceleration is actually an inverse problem, which can be solved more easily by transforming equation (1) from the angular time domain to the angular frequency domain:

$$T_p(\lambda) = T_e(\lambda) + T_r(\lambda) + T_L(\lambda)$$
$$= \tfrac{1}{2} i\lambda X(\lambda)[H(\lambda)]^{-1} + T_r(\lambda) + T_L(\lambda) \qquad (2)$$

where λ is the variable in the angular frequency domain corresponding to the variable θ in the crankshaft angular domain, $T_p(\lambda)$, $T_e(\lambda)$, $T_r(\lambda)$ and $T_L(\lambda)$ are the Fourier transforms of $T_p(\theta)$, $T_e(\theta)$, $T_r(\theta)$ and $T_L(\theta)$ respectively, $H(\lambda)$ is the Fourier transform of $h(\theta)$ acting as the transfer function of the system, $X(\lambda)$ is the Fourier transform of $x(\theta) = [\omega(\theta)]^2$ and $i = \sqrt{-1}$. Note that the equality $T_e(\lambda) = \tfrac{1}{2} i\lambda X(\lambda)[H(\lambda)]^{-1}$ is obtained from the differentiation property of Fourier transform, i.e. the Fourier transform of $dx(\theta)/d\theta$ is $i\lambda X(\lambda)$, and the relationship between angular acceleration and angular velocity in the θ domain:

$$\alpha(\theta) = \alpha(t) = \frac{d\omega(t)}{dt} = \frac{d\omega[\theta(t)]}{dt} = \frac{d\omega(\theta)}{d\theta} \frac{d\theta(t)}{dt}$$
$$= \frac{d\omega(\theta)}{d\theta} \omega(\theta) = \frac{1}{2} \frac{d[\omega(\theta)]^2}{d\theta} = \frac{1}{2} \frac{dx(\theta)}{d\theta} \qquad (3)$$

In equation (2), both $T_r(\lambda)$ and $T_L(\lambda)$ can be pre-calculated because $T_r(\theta)$ is purely deterministic and completely described by engine geometry and $T_L(\theta)$ is assumed constant. Therefore, once a data block of $\omega(\theta)$, sampled at discrete evenly spaced crankshaft intervals or sampled in the θ domain, is obtained, $X(\lambda)$ will be directly computed by the discrete Fourier transform (DFT) of the square of this data block, giving an estimate of gas pressure torque $T_p(\lambda)$ in the λ domain.

2.2 Feature extraction based on gas pressure torque estimation

There are two methods that can be used to calculate $T_p(\lambda)$ in the λ domain by equation (3), which lead to the development of different fast algorithms of feature extraction for engine misfire detection. The first method is performed at harmonics of the engine cycle frequency, denoted by λ_c, providing a set of components of $T_p(\lambda)$ for each engine cycle, and thus the calculation is based on the entire data block in each engine cycle. If the engine runs normally with cylinder-to-cylinder uniformity, the component of $T_p(\lambda)$ corresponding to the firing frequency is much larger in amplitude than those below the firing frequency. However, if cylinder-to-cylinder non-uniformity (e.g. misfire) happens in the engine, the harmonic components of $T_p(\lambda)$ below the firing frequency will increase significantly. Because this property has been noticed, a dimensionless feature to detect misfire for the entire engine has been defined and it is called

the torque component ratio:

$$R_T = \frac{\sqrt{\sum_{m=1}^{N-1} |T_p(m\lambda_c)|^2}}{|T_p(N\lambda_c)|} \qquad (4)$$

where N is the number of engine cylinders and $T_p(m\lambda_c)$ represents the gas pressure torque component at the mth harmonic within each engine cycle.

The second method for $T_p(\lambda)$ calculation is performed at harmonics of the engine firing frequency, denoted by λ_f, giving a set of components of $T_p(\lambda)$ for each cylinder within each engine cycle, and thus the calculation is made from each data block corresponding to each individual cylinder. As the cylinder-to-cylinder fluctuation of the gas pressure torque indicates the power generation capability of each individual cylinder, the torque output of each cylinder will be almost equal if the engine runs under a normal cylinder-to-cylinder uniform condition. Nevertheless, if misfire happens in a certain cylinder, the torque output of this cylinder will decrease significantly. For this reason, another dimensionless feature to detect misfire for the nth individual cylinder has been defined and it is called the torque fluctuation index:

$$I_T^{(n)} = \frac{\bar{T}_p^{(n)}}{\frac{1}{N} \sum_{n=1}^{N} \bar{T}_p^{(n)}} \qquad (5)$$

where $\bar{T}_p^{(n)}$ is a parameter reflecting the gas pressure torque output of the nth cylinder, and it can be estimated from the root mean square (r.m.s.) value of the lower frequency components, i.e.

$$\bar{T}_p^{(n)} = \frac{1}{K} \sqrt{\sum_{m=1}^{K} |\bar{T}_p^{(n)}(m\lambda_f)|^2} \qquad (6)$$

where $T_p^{(n)}(m\lambda_f)$ represents the gas pressure torque component at the mth frequency harmonic $m\lambda_f$ for the nth cylinder within each engine cycle and K is the number of harmonics of λ_f utilized. K can be determined using knowledge of the combustion pressure as it propagates through the engine dynamics to cause angular velocity fluctuations. For example, if the assumption is made that most of the energy in the fluctuating gas pressure torque is contained in the first three harmonics of λ_f, then $K = 3$ is sufficient to estimate $\bar{T}_p^{(n)}$.

Let L be the number of angular velocity samples per engine cycle and $\{\omega_k: k = 0, 1, 2, \ldots, L-1\}$ be the data block of angular velocity samples per engine cycle. Then, according to equations (2) and (4), the calculation of the feature R_T only requires N components of $X(\lambda)$ at lower frequency harmonics within one engine cycle, which can be obtained quickly by DFT:

$$X(m\lambda_c) = \sum_{k=0}^{L-1} \omega_k^2 e^{-i2\pi mk/L}, \qquad m = 1, 2, \ldots, N \qquad (7)$$

Let $\{\omega_k^n: k = 0, 1, 2, \ldots, L/N-1; n = 1, 2, \ldots, N\}$ be the data block of angular velocity samples per cylinder per engine cycle. Then, according to equations (2), (5) and (6), the calculation of the feature $I_T^{(n)}$ only requires K components of $X(\lambda)$ at lower frequency harmonics for the nth cylinder in an engine cycle, which can be achieved quickly by DFT:

$$X^{(n)}(m\lambda_f) = \sum_{k=0}^{M-1} [\omega_k^{(n)}]^2 e^{-i2\pi mk/M}, \qquad m = 1, 2, \ldots, K \qquad (8)$$

The calculation of the features R_T and $I_T^{(n)}$ requires knowledge of the engine transfer function $X(\lambda)$ that is determined by the engine structural parameters. However, it is usually not easy to obtain such structural parameters for some engines. In this case, by neglecting the influence of the reciprocating torque components $T_r(\lambda)$ and by considering $A(\lambda)$ as the estimate of $T_p(\lambda)$, two other similar dimensionless features have been defined for engine misfire detection: acceleration component ratio, R_F, and acceleration fluctuation index, $I_F^{(n)}$:

$$R_F = \frac{\sqrt{\sum_{n=1}^{N-1} |A(n\lambda_c)|^2}}{|A(N\lambda_c)|} \qquad (9)$$

$$I_F^{(n)} = \frac{\bar{A}^{(n)}}{\frac{1}{N} \sum_{n=1}^{N} \bar{A}^{(n)}} \qquad (10)$$

where $A(n\lambda_c)$ represents the angular acceleration component at the nth frequency harmonic $n\lambda_c$ within each engine cycle and $\bar{A}^{(n)}$ is an estimate reflecting the angular acceleration fluctuation of the nth cylinder.

2.3 Feature extraction based on waveform analysis

According to equation (3), the instantaneous angular acceleration $\alpha(\theta)$ can be easily calculated from the measurements of instantaneous angular velocity $\omega(\theta)$. Figure 1 depicts the waveforms of $\alpha(\theta)$ and $\omega(\theta)$ measured from a four-cylinder four-stroke diesel engine (see Table 1) with cylinder 3 misfiring and filtered by the fast Fourier transform filtering method.

As previously discussed, $\alpha(\theta)$ is proportional to the engine rotating torque $T_e(\theta)$. Thus $\alpha(\theta)$ would be proportional to the fluctuating component of the gas pressure torque $T_p(\theta)$ if the influences of the reciprocating torque $T_r(\theta)$ and the resistive torque $T_L(\theta)$ were to be neglected. This helps directly to define three dimensionless features from the angular acceleration waveform for the misfire detection of an individual cylinder. These have been called the maximum acceleration index, $I_H^{(n)}$, minimum acceleration index, $I_L^{(n)}$, and summed
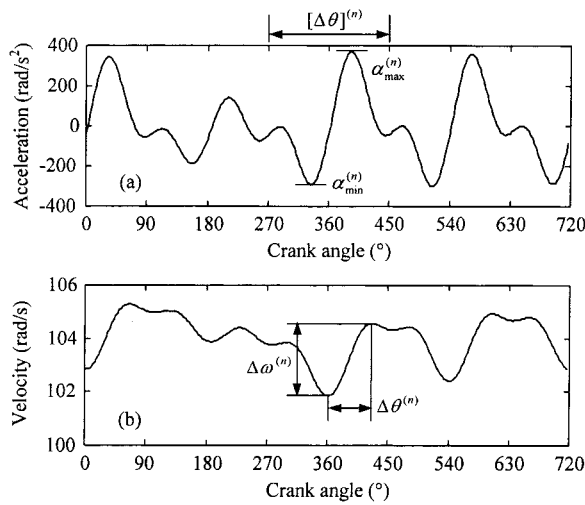
Fig. 1 Waveforms of (a) instantaneous angular acceleration and (b) instantaneous angular velocity during a cycle in a four-cylinder four-stroke engine

Table 1 Specification of the test engine

Engine type	Model 4135D, 8.6 l, 4-cylinder, 4-stroke, direct injection diesel
Manufacturer	Shanghai Diesel Works
Bore × stroke	135 mm × 150 mm
Maximum power output	123.6 kW at 1500 r/min
Maximum torque	582 N m at 1200 r/min
Compression ratio	17:1
Firing order	1–3–4–2 (from timing cover)

acceleration index, $I_S^{(n)}$:

$$I_H^{(n)} = \frac{\alpha_{max}^{(n)}}{\frac{1}{N}\sum_{n=1}^{N}\alpha_{max}^{(n)}} \tag{11}$$

$$I_L^{(n)} = \frac{\alpha_{min}^{(n)}}{\frac{1}{N}\sum_{n=1}^{N}\alpha_{min}^{(n)}} \tag{12}$$

$$I_S^{(n)} = \frac{\alpha_{sum}^{(n)}}{\frac{1}{N}\sum_{n=1}^{N}\alpha_{sum}^{(n)}} = \frac{\int_{[\Delta\theta]^{(n)}}|\alpha(\theta)|\,d\theta}{\frac{1}{N}\sum_{n=1}^{N}\int_{[\Delta\theta]^{(n)}}|\alpha(\theta)|\,d\theta} \tag{13}$$

where $\alpha_{max}^{(n)}$, $\alpha_{min}^{(n)}$ and $\alpha_{sum}^{(n)}$ are respectively the peak value, the valley value and the summed absolute value of the angular acceleration waveform of the nth cylinder and $[\Delta\theta]^{(n)}$ is the crankshaft angular interval corresponding to the nth cylinder.

As shown in Fig. 1b, in the waveform of instantaneous angular velocity there exists an acceleration during the expansion stroke of each cylinder because of the combustion pressure force. Let $\omega_{max}^{(n)}$ and $\omega_{min}^{(n)}$ be respectively the peak value and valley value of the angular velocity waveform during the expansion stroke of the nth cylinder and $\theta_{max}^{(n)}$ and $\theta_{min}^{(n)}$ be their corresponding crankshaft

angular positions. Then, the maximum variation in the instantaneous angular velocity, $\Delta\omega^{(n)} = \omega_{max}^{(n)} - \omega_{min}^{(n)}$, and its corresponding angular duration, $\Delta\theta^{(n)} = \theta_{max}^{(n)} - \theta_{min}^{(n)}$, are both indicators of the mean gas pressure torque of the nth cylinder. Therefore, three features can be defined to identify whether the nth cylinder is misfiring. They are called the angular variation index $I_C^{(n)}$, velocity variation index, $I_V^{(n)}$ and acceleration variation index, $I_A^{(n)}$:

$$I_C^{(n)} = \frac{\Delta\theta^{(n)}}{\frac{1}{N}\sum_{n=1}^{N}\Delta\theta^{(n)}} \tag{14}$$

$$I_V^{(n)} = \frac{\Delta\omega^{(n)}}{\frac{1}{N}\sum_{n=1}^{N}\Delta\omega^{(n)}} \tag{15}$$

$$I_A^{(n)} = \frac{\frac{\Delta\omega^{(n)}}{\Delta\theta^{(n)}}}{\frac{1}{N}\sum_{n=1}^{N}\frac{\Delta\omega^{(n)}}{\Delta\theta^{(n)}}} \tag{16}$$

3 ON-LINE MISFIRE DETECTION BY MULTIPLE FEATURE FUSION

3.1 Misfire detection by each individual feature

So far 10 dimensionless features have been defined along with fast feature extraction algorithms. Here rules are presented for each individual feature to identify engine misfire. Among these rules, rule 1 is for R_T and R_F and rules 2–4 are for $I_T^{(n)}$, $I_F^{(n)}$, $I_H^{(n)}$, $I_L^{(n)}$, $I_S^{(n)}$, $I_C^{(n)}$, $I_V^{(n)}$ and $I_A^{(n)}$.

Taking R_T as an example, rule 1 for a selected threshold $R_{T,0}$ would be

Rule 1

IF $R_T \leqslant R_{T,0}$
THEN all cylinders are healthy
ELSE one or more cylinders is misfiring

Taking $I_T^{(n)}$ as an example, rules 2–4 for a selected value ε are as follows. Here ε is a minor positive value quite near zero. Its introduction is to distinguish the normally acceptable cylinder-to-cylinder non-uniformity from the abnormal misfire and thus to avoid a mistaken diagnosis.

Rule 2

IF $1 - \varepsilon \leqslant I_T^{(n)} \leqslant 1 + \varepsilon$ for all cylinders
THEN all cylinders are healthy

Rule 3

IF $I_T^{(n)} < 1 - \varepsilon$
THEN the nth cylinder is misfiring

Rule 4

IF $I_T^{(n)} > 1 + \varepsilon$
Then the nth cylinder is healthy while misfire exists in
another cylinder or cylinders

3.2 On-line misfire detection by multiple feature fusion

According to rule 1, among the 10 dimensionless features, neither R_T nor R_F is capable of identifying the misfiring cylinder(s), but both of them can detect whether the engine is healthy or faulty with much simpler computations. According to rules 2–4, on the contrary, all of the other eight features have the capability to identify the individual misfiring cylinder(s) but with more complex computations. For this reason, a technique for the on-line detection of engine misfire has been proposed which aims at achieving improved diagnostic efficiency and reliability.

The technique is depicted in Fig. 2, where all of the 10 dimensionless features are used. If the engine structural parameters are known, R_T will identify whether the engine is healthy or faulty at first and $I_T^{(n)}$ will then locate the position of a misfiring cylinder or cylinders if necessary. Otherwise, if the engine structural parameters are unknown, R_F will detect whether the engine is healthy, and the remaining seven features can then be used to identify the possible misfiring cylinder(s). The technique involves a multiple feature fusion process, which is based on the feature level fusion architecture for multisensor fusion [20] but with some modification.

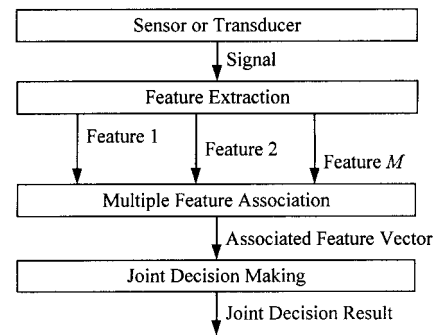As illustrated in Fig. 3, not multisensors but only a

Fig. 3 Proposed architecture of multiple feature fusion

single sensor provides the data (i.e. the instantaneous angular velocity signal), from which several single features are extracted by different feature extraction approaches. Then these features are associated together into a single feature vector, which in turn is input to a decision-making procedure, which may be a neural network or clustering algorithm. Noticing that the decision making is in fact a process of pattern recognition; here a fuzzy pattern recognition technique [21] is introduced, which is particularly suitable for the association of multiple dimensionless features. The principles are demonstrated in the following section.

4 MULTIPLE FEATURE FUSION PROCEDURE

4.1 Principles of fuzzy pattern recognition

The problem of fuzzy pattern recognition can be simply described as follows [21]: given K known patterns,
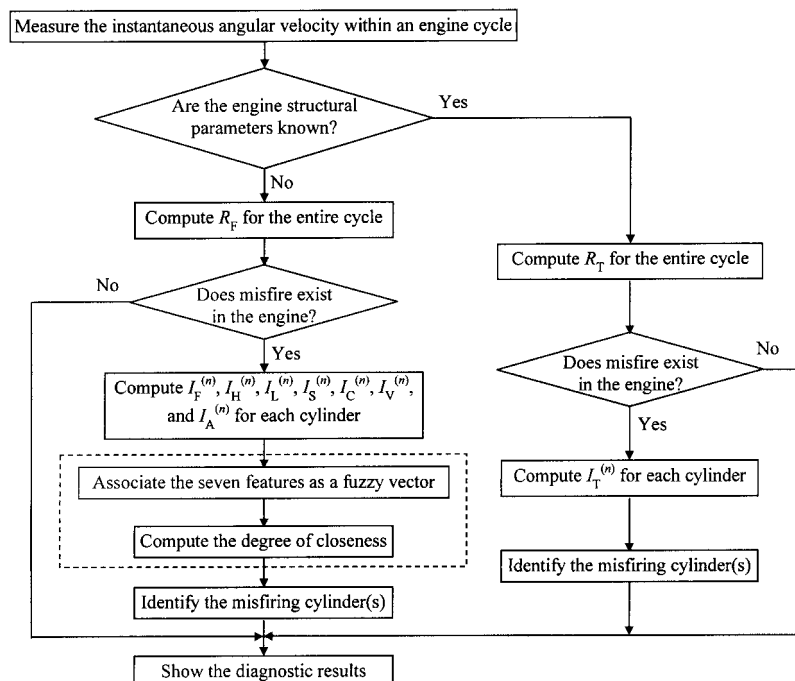

Fig. 2 Proposed technique for on-line detection of engine misfire based on multiple feature fusion

A_1, A_2, .., A_K, and one new pattern, B, identify which known pattern the new pattern should be classified into. In this description, each pattern, denoted by A, is a fuzzy vector

$$A = (a_1, a_2, \ldots, a_M) \qquad (17)$$

where each element of the vector, a_m, satisfies

$$0 \leqslant a_m \leqslant 1, \qquad m = 1, 2, \ldots, M \qquad (18)$$

The fuzzy vector A can be interpreted as a fuzzy set in the domain $U = [u_1, u_2, \ldots, u_M\}$

$$A = \left\{ \frac{a_1}{u_1}, \frac{a_2}{u_2}, \ldots, \frac{a_M}{u_M} \right\} \qquad (19)$$

where the transformation of a_m to u_m is often termed fuzzification [22], which depends on a membership function

$$a_m = \mu(u_m) \qquad (20)$$

Once all of the known patterns and the new pattern have been represented as fuzzy vectors, the pattern recognition can be achieved by computing and comparing the degree of closeness between the new fuzzy vector B and each known fuzzy vector A_k ($k = 1, 2, \ldots, K$). If there is a known vector A_j with $j \in \{1, 2, \ldots, K\}$ satisfying

$$\sigma(B, A) = \max_{1 \leqslant k \leqslant M} (B, A_k) \qquad (21)$$

then B is the nearest to A_j among all of the known patterns, that is to say the new pattern B should be classified into the known pattern A_j. This is called the nearest selection criterion in fuzzy pattern recognition.

In equation (21), σ is called the degree of closeness between two fuzzy vectors [21]. Although there are many definitions for the degree of closeness, each of them is generally intended for a particular purpose. Here two definitions are used for engine misfire detection:

1. Maximum–minimum degree of closeness σ_1

$$\sigma_1(A, B) = \frac{\displaystyle\sum_{m=1}^{M} \min(a_m, b_m)}{\displaystyle\sum_{m=1}^{M} \max(a_m, b_m)} \qquad (22)$$

2. Euclidean distance degree of closeness σ_2

$$\sigma_2(A, B) = 1 - \sqrt{\frac{1}{M} \sum_{m=1}^{M} (a_m, b_m)^2} \qquad (23)$$

where $A = (a_1, a_2, \ldots, a_M)$ and $B = (b_1, b_2, \ldots, b_M)$ are two fuzzy vectors.

4.2 Misfire detection by multiple feature fusion with fuzzy pattern recognition

As depicted in Fig. 2, if the engine structural parameters are unknown, whether an individual cylinder is healthy or misfiring will be identified not by a single feature but

by seven features together, $I_F^{(n)}$, $I_H^{(n)}$, $I_L^{(n)}$, $I_S^{(n)}$, $I_C^{(n)}$, $I_V^{(n)}$ and $I_A^{(n)}$. This is achieved by fuzzy pattern recognition with the following procedure:

1. The seven features of each individual cylinder are associated together as a vector:

$$U^{(n)} = (u_1^{(n)}, u_2^{(n)}, u_3^{(n)}, u_4^{(n)}, u_5^{(n)}, u_6^{(n)}, u_7^{(n)})$$
$$= (I_F^{(n)}, I_H^{(n)}, I_L^{(n)}, I_S^{(n)}, I_C^{(n)}, I_V^{(n)}, I_A^{(n)}) \qquad (24)$$

2. $U^{(n)}$ is transformed into a fuzzy vector

$$B^{(n)} = (b_1^{(n)}, b_2^{(n)}, b_3^{(n)}, b_4^{(n)}, b_5^{(n)}, b_6^{(n)}, b_7^{(n)})$$

with each element $u_m^{(n)}$ ($m = 1, 2, \ldots, 7$) of $U^{(n)}$ being fuzzified by the uphill distribution member function (its property is shown in Fig. 4)

$$b_m^{(n)} = \mu(u_m^{(n)})$$

$$= \begin{cases} 0, & 0 \leqslant u_m^{(n)} < d_m \\[4pt] \dfrac{1}{2} + \dfrac{1}{2} \sin\left[\dfrac{\pi}{c_m - d_m} \right. \\[8pt] \qquad \left. \times \left(u_m^{(n)} - \dfrac{c_m + d_m}{2} \right) \right], & d_m < u_m^{(n)} < c_m \\[8pt] 1, & u_m^{(n)} \geqslant c_m \end{cases} \qquad (25)$$

where c_m and d_m are both constant and can be determined by the relationship of $u_m^{(n)}$ among N cylinders:

$$c_m = \max_{1 \leqslant n \leqslant N} (u_m^{(n)})$$
$$d_m = \frac{1}{3} c_m \qquad (26)$$

3. The degree of closeness σ_1 (or σ_2) is calculated between the new fuzzy vector $B^{(n)}$ and a standard known fuzzy vector A. This standard vector A is defined under a healthy engine condition with absolute cylinder-to-cylinder uniformity. Under such a condition, all of the seven features, $I_F^{(n)}$, $I_H^{(n)}$, $I_L^{(n)}$, $I_S^{(n)}$, $I_C^{(n)}$, $I_V^{(n)}$ and $I_A^{(n)}$, should theoretically be unity for all of the N cylinders, and their fuzzified values should still be unity. Therefore, the standard vector A of all cylinders can have the form

$$A = (1, 1, 1, 1, 1, 1, 1) \qquad (27)$$

4. The following rule identifies whether the nth cylinder is healthy or misfiring, where σ_0 is a dimensionless
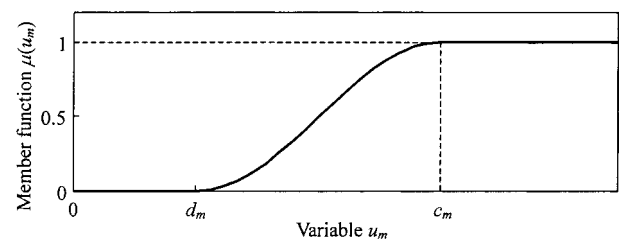

Fig. 4 Uphill distribution membership function

threshold and may be statistically determined from experimental data.

Rule 5

IF $\sigma_1 \geqslant \sigma_0$ (or $\sigma_2 \geqslant \sigma_0$)
THEN the nth cylinder is healthy
ELSE the nth cylinder is misfiring

5   EXPERIMENTAL RESULTS AND DISCUSSION

5.1   Measured signals from a production engine

To obtain instantaneous angular velocity signals to validate the proposed on-line misfire detection technique, an engine test facility was set up. The specification of the test engine, a model 4135D four-cylinder four-stroke diesel engine, produced by Shanghai Diesel Works and used in light commercial vehicles, is given in Table 1. The engine was loaded with a hydraulic dynamometer and was appropriately instrumented to record the operating parameters. To allow the proposed technique to be validated over a wide range of engine operation conditions, the measurement of instantaneous angular velocity was performed over a selection of speed and load settings.

An eddy current displacement sensor mounted opposite the flywheel was used to measure instantaneous angular velocity signal, and a Hall effect device on the camshaft provided a timing reference point at the top dead centre (TDC) of cylinder 1. This device had the characteristic that the angular velocity resolution decreases as the engine speed increases. A personal computer (PC) mounted with a Real Time Devices AD3110 analogue-to-digital conversion data acquisition (DAQ) board was used for data collection and analysis. As the flywheel had 128 teeth and the AD3110 DAQ board provided a timer counter of 8 MHz clock rate, the minimum angular velocity resolution was 0.6 r/min at the highest engine speed of 1500 r/min. This resolution is, however, considered sufficient for misfire detection, since the angular velocity variation observed was more than 20 r/min even with the engine running in a healthy condition under very low load.

Figures 5 to 8 present waveforms of instantaneous angular velocity measured under the same load of 30 N m over a range of operating conditions (i.e. without misfiring, with cylinder 3 misfiring, with cylinders 2 and 3 spatially misfiring, and with cylinders 3 and 4 sequentially misfiring). Each figure includes four plots corresponding to mean engine speeds of 700, 1000, 1200 and 1500 r/min. Two cycles of sampled data are depicted in each plot and the x coordinate represents the crankshaft angular position relative to the TDC of cylinder 1.
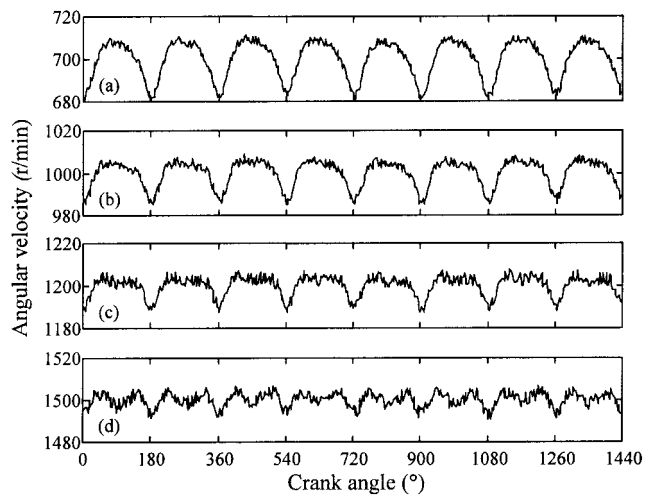

Fig. 5 Measured instantaneous angular velocity without misfire for mean engine speeds of (a) 700, (b) 1000, (c) 1200 and (d) 1500 r/min
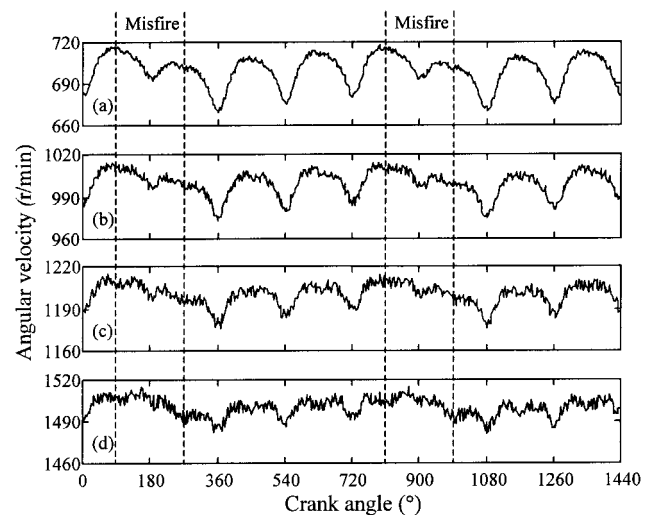

Fig. 6 Measured instantaneous angular velocity with cylinder 3 misfiring for mean engine speeds of (a) 700, (b) 1000, (c) 1200 and (d) 1500 r/min

5.2   Misfire detection capability by each individual feature

Figure 9 shows the calculated features R_T and R_F for the range of operating conditions as described in Figs 5 to 8. It is clear that the calculated values of these two features for a healthy engine are almost 10 times as great as those for a faulty engine. Therefore, the features R_T and R_F can easily detect whether misfire exits in the engine, although, as previously explained, neither can identify which cylinder is misfiring. It is also observed that the influence of the engine speed, especially higher speeds, should be considered carefully when using the feature R_F, but this caution is not necessary for the feature R_T.

Figures 10 and 11 depict the calculated values of the other eight features for engine speeds of 1000 and
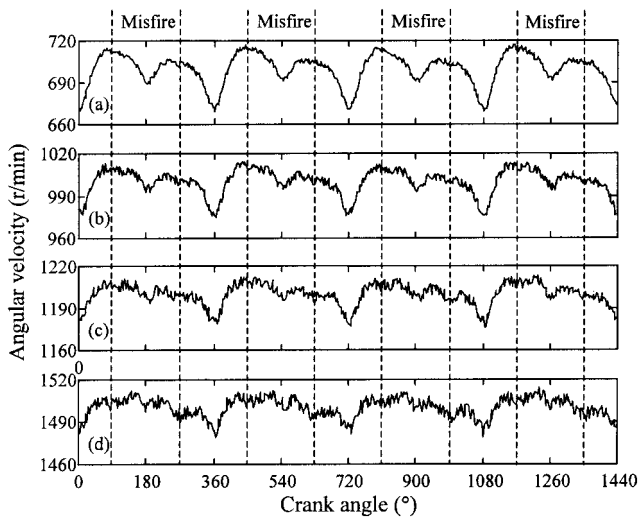
Fig. 7 Measured instantaneous angular velocity with cylinders 2 and 3 spatially misfiring for mean engine speeds of (a) 700, (b) 1000, (c) 1200 and (d) 1500 r/min
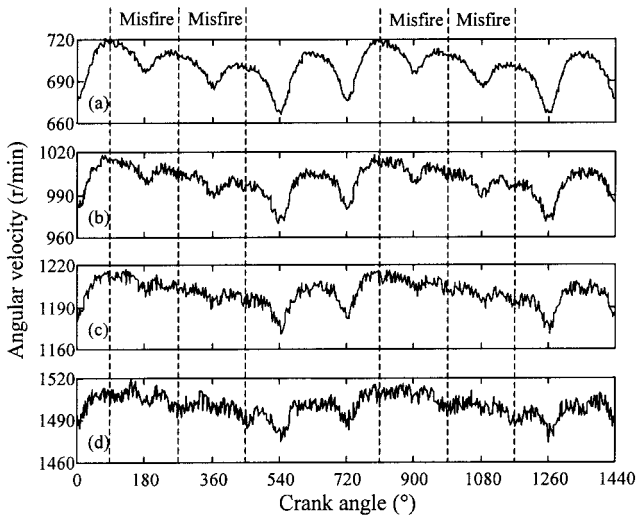

Fig. 8 Measured instantaneous angular velocity with cylinders 3 and 4 sequentially misfiring for mean engine speeds of (a) 700, (b) 1000, (c) 1200 and (d) 1500 r/min
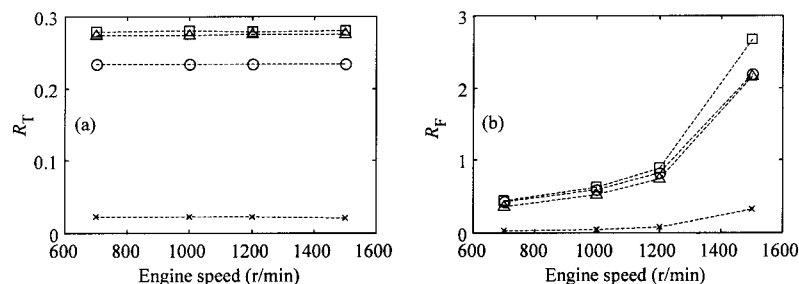
1500 r/min under the same range of conditions as described in Figs 5 to 8. It is observed that all these features have the capability of both detecting engine misfire and locating its position. Among the eight features $I_{\mathrm{T}}^{(n)}$ is observed to be more accurate for identifying the misfiring cylinder(s) than the other seven features, but its computation is more complex since it requires knowledge of engine structural parameters. Some features, particularly $I_{\mathrm{C}}^{(n)}$, $I_{\mathrm{V}}^{(n)}$ and $I_{\mathrm{A}}^{(n)}$, which are directly extracted from the angular velocity waveform, could not be calculated under certain engine conditions. This occurs when there is no obvious acceleration in the angular velocity waveform and especially at high engine speeds or a certain cylinder is misfiring. As shown in Fig. 11, these features are fixed at zero in such cases, but this simple adjustment may possibly give an erroneous diagnosis.

It is interesting to note that the diagnostic conclusions implied by different single features do not always concur and sometimes they directly conflict with one another. For example, the feature $I_{\mathrm{A}}^{(n)}$ would give an erroneous diagnostic decision with the engine at 1500 r/min when cylinders 3 and 4 both misfire (shown in Fig. 11), whereas other features can detect this fault correctly. This indicates that the information provided by multiple features is usually redundant and complementary, but sometimes contradictory, and one single feature may hence simply not be sufficient to make a reliable misfire decision.

5.3 Misfire detection capability by multiple feature fusion

Since the forcing of incomputable features to be zero increases the probability of an erroneous diagnosis, a feature selection process can be performed before the multiple feature fusion procedure described in section 4.2. This can be achieved by excluding the incomputable features from the feature vector shown in equation (24). For example, if three features $I_{\mathrm{C}}^{(n)}$, $I_{\mathrm{V}}^{(n)}$ and $I_{\mathrm{A}}^{(n)}$ are incomputable, the fuzzy vector of the nth cylinder

Fig. 9 Calculated features R_{T} and R_{F} at speeds of 700–1500 r/min ($\times$, without misfire; #, with cylinder 3 misfiring; , with cylinders 2 and 3 misfiring; %, with cylinders 3 and 4 misfiring)
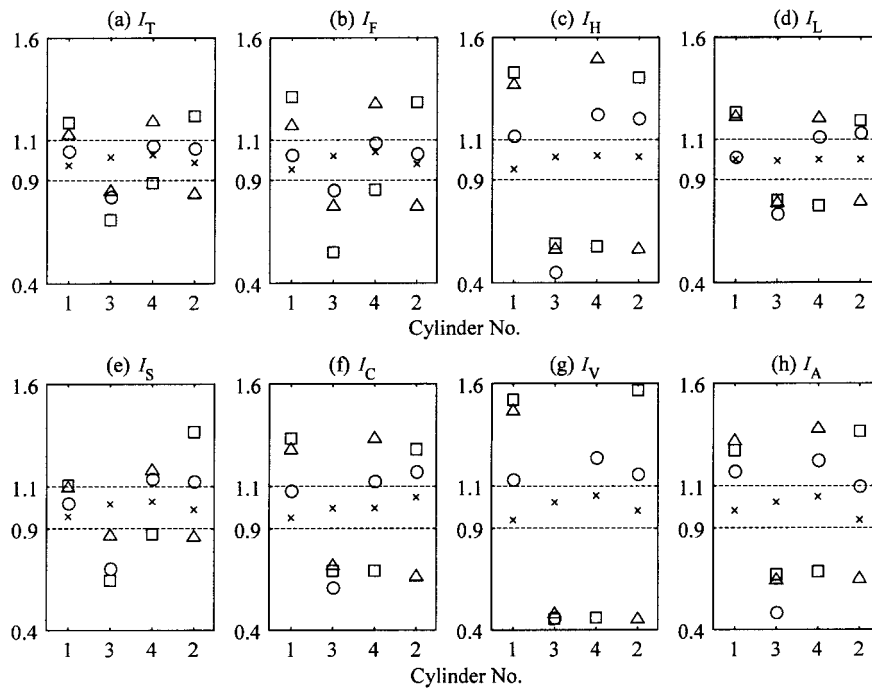
Fig. 10 Calculated features $I_T^{(n)}$, $I_F^{(n)}$, $I_H^{(n)}$, $I_L^{(n)}$, $I_S^{(n)}$, $I_C^{(n)}$, $I_V^{(n)}$ and $I_A^{(n)}$ at a speed of 1000 r/min ($\times$, without misfire; #, with cylinder 3 misfiring; , with cylinders 2 and 3 misfiring; %, with cylinders 3 and 4 misfiring)
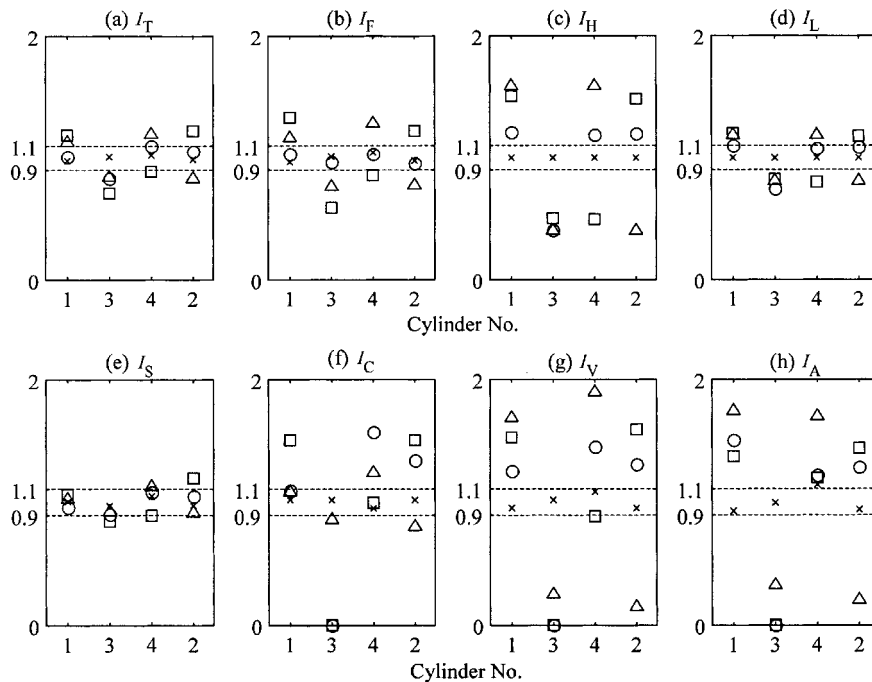

Fig. 11 Calculated features $I_T^{(n)}$, $I_F^{(n)}$, $I_H^{(n)}$, $I_L^{(n)}$, $I_S^{(n)}$, $I_C^{(n)}$, $I_V^{(n)}$ and $I_A^{(n)}$ at a speed of 1500 r/min ($\times$, without misfire; #, with cylinder 3 misfiring; , with cylinders 2 and 3 misfiring; %, with cylinders 3 and 4 misfiring)

would be $\boldsymbol{B}^{(n)} = (\mu[I_F^{(n)}], \mu[I_H^{(n)}], \mu[I_L^{(n)}], \mu[I_S^{(n)}])$, which contains only four elements. Meanwhile, the standard vector in equation (27) would become $\boldsymbol{A} = (1, 1, 1, 1)$. Then the degree of closeness σ_1 or σ_2 between the new vector $\boldsymbol{B}^{(n)}$

and the standard vector $\boldsymbol{A}$ will identify whether the nth cylinder is misfiring.

Figure 12 presents σ_1 and σ_2 calculated by the proposed multiple feature fusion technique, with the engine
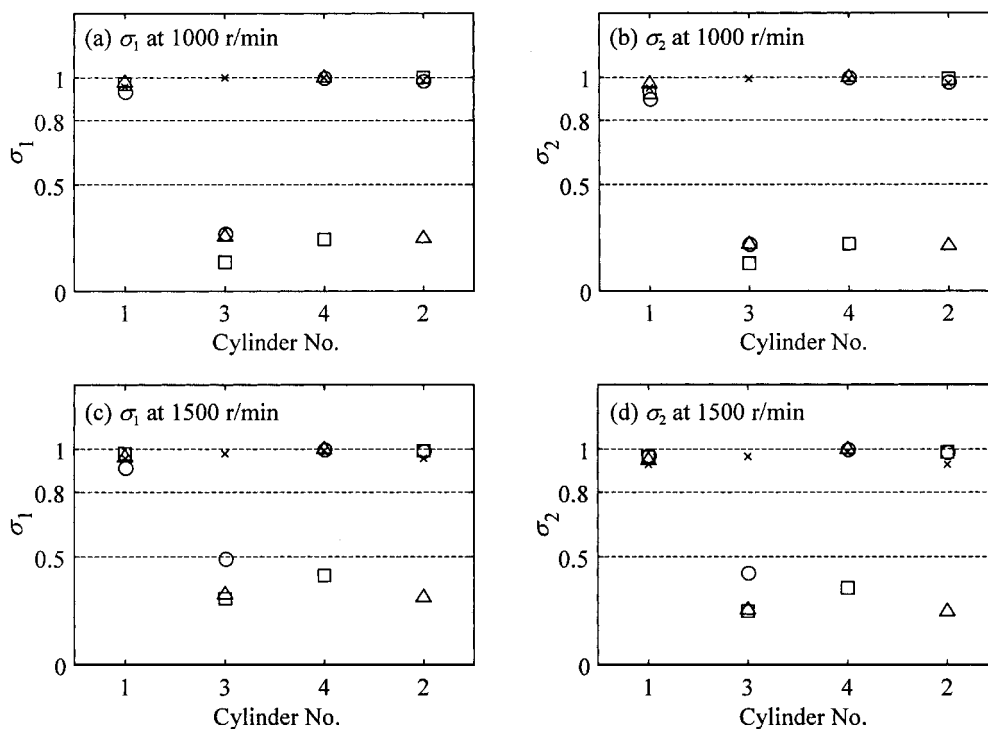
Fig. 12 Calculated degrees of closeness σ_1 and σ_2 at speeds of 1000 and 1500 r/min ($\times$, without misfire; #, with cylinder 3 misfiring; , with cylinders 2 and 3 misfiring; %, with cylinders 3 and 4 misfiring)

at 1000 and 1500 r/min and under the same range of conditions as described in Figs 5 to 8. It is observed that all these values are less than 0.5 for a misfiring cylinder but more than 0.8 for a healthy cylinder. This difference is so distinct that the selection of a threshold for σ_1 or σ_2 is much more straightforward than for a single feature.

It is also noted that the proposed multiple feature fusion technique exploits the redundant and complementary information of all the single features and thus leads to improved diagnostic reliability. For example, the proposed technique can identify the misfiring cylinders 3 and 4 correctly with the engine at 1500 r/min. This is important because such a conclusion is obtained when the individual feature $I_A^{(n)}$ gives an erroneous diagnosis (shown in Fig. 11). A similar case can be seen when the engine ran at 1500 r/min with cylinder 3 misfiring.

As described in Fig. 2, only after a data block of instantaneous angular velocity within one engine cycle is available will the PC system start to analyse the data, calculate the features and, finally, draw a conclusion on whether the engine is healthy and which cylinder is misfiring. This indicates that the proposed technique for engine misfire detection is on a cycle-by-cycle basis. In this study, without knowledge of the engine structural parameters, the total computation time during one engine cycle is 5.7 ms when using a PC system with an Intel Pentium 10 MHz CPU and 32M RAM running under Microsoft Windows 95. Obviously this computation time is much shorter than the duration of one

engine cycle, which is, for instance, 80 ms with the four-stroke engine at 1500 r/min. From this point of view, the proposed algorithms are verified to be fast in computation and have the potential capability for on-line monitoring and real-time diagnosis of engine misfire.

6 SUMMARY AND CONCLUSIONS

In this paper, a technique for the on-line detection of engine misfire based on multiple feature fusion has been proposed. Ten dimensionless features with fast computational algorithms have been defined and if all these features are associated together they can firstly identify reliably whether the engine is healthy or misfiring and secondly locate the position of a misfiring cylinder or cylinders.

Although all of the single features can be used to detect misfire, none of these features is found to be universally successful because of the complex nature of the in-cylinder process. The diagnostic results from single features are not always concurrent and sometimes actually conflict with one another.

The fusion of multiple features has been demonstrated to provide significant advantages over the use of single features. In this way it exploits the redundant and complementary information of all the features and thus leads to improved diagnostic reliability.

The proposed multiple feature technique has been proven to be simple in implementation and fast in com-

putation, and it may hence provide a basis for a practical utility in on-line monitoring and real-time diagnosis of engine misfire.

Owing to the limitation that the maximum speed of the test engine is only 1500 r/min, further work is still to be undertaken on other high speed engines so that the proposed technique will also be effective in high speed conditions.

ACKNOWLEDGEMENT

REFERENCES

1 **Sood, A. K., Fahs, A. A.** and **Henein, N. A.** A real-time microprocessor-based system for engine deficiency analysis. *IEEE Trans. Ind. Electronics*, 1983, **30**(2), 159–163.

2 **William, P.** and **Stephen, J.** An on-line engine roughness measurement technique. SAE paper 840136, 1984.

3 **Ribbens, W. B.** and **Rizzoni, G.** Application of precise crankshaft position measurements for engine testing, control and diagnosis. SAE paper 890885, 1989.

4 **Kao, M.** and **Moskwa, J. J.** Nonlinear diesel engine control and cylinder pressure observation analysis. *Trans. ASME, J. Dynamic Systems, Measmt, Control*, 1995, **117**(2), 183–192.

5 **Sood, A. K., Friedlander, C. B.** and **Fahs, A. A.** Engine fault analysis: I—statistical method. *IEEE Trans. Ind. Electronics*, 1985, **32**(4), 294–300.

6 **Freestone, J. W.** and **Jenkins, E. G.** The diagnosis of cylinder power faults in a diesel engine by flywheel speed measurement. *Proc. Instn Mech. Engrs*, 1986, **200**(D1), 37–43.

7 **Henein, N. A., Bryzik, W., Taylor, C.** and **Nichols, A.** Dynamic parameters for engine diagnostics: effect of sampling. SAE paper 932411, 1993.

8 **Jewitt, T. H. B.** and **Lawton, R.** The use of speed sensing for monitoring the condition of military vehicle engines. *Proc. Instn Mech. Engrs*, 1986, **200**(D1), 45–51.

9 **Rezeka, S. F.** and **Henein, N. A.** A diagnostic technique for the identification of misfiring cylinder(s). SAE paper 870546, 1987.

10 **Citron, S. J., O'Higgins, J. E.** and **Chen, L. Y.** Cylinder by cylinder engine pressure and pressure torque waveform determination utilizing speed fluctuations. SAE paper 890486, 1989.

11 **Mauer, G. F.** On-line cylinder fault diagnostics for internal combustion engines. *IEEE Trans. Ind. Electronics*, 1990, **37**(3), 221–226.

12 **Rizzoni, G.** and **Connolly, F. T.** Estimation of IC engine torque from measurement of crankshaft angular position. SAE paper 932410, 1993.

13 **Shiao, Y.** and **Moskwa, J. J.** Misfire detection and cylinder pressure reconstruction for SI engines. SAE paper 940144, 1994.

14 **Connolly, F. T.** and **Yagle, A. E.** Modelling and identification of the combustion pressure process in internal combustion engines. *Mech. Systems Signal Processing*, 1994, **8**(1), 1–19.

15 **Rizzoni, G.** and **Zhang, Y.** Identification of a non-linear internal combustion engine model for on-line indicated torque estimation. *Mech. Systems Signal Processing*, 1994, **8**(3), 275–287.

16 **Connolly, F. T.** and **Rizzoni, G.** Real-time estimation of engine torque for the detection of engine misfires. *Trans. ASME, J. Dynamic Systems, Measmt, Control*, 1994, **116**(4), 675–686.

17 **Shiao, Y.** and **Moskwa, J. J.** Cylinder pressure and combustion heat release estimation for SI engine diagnostics using non-linear sliding observers. *IEEE Trans. Control Systems Technol.*, 1995, **3**(1), 70–78.

18 **Luo, R. C.** and **Kay, M. G.** Multisensor integration and fusion in intelligent systems. *IEEE Trans. Systems, Man Cybernetics*, 1989, **19**(4), 901–931.

19 **Dasarathy, B. V.** Paradigms for information processing in multisensor environments. *Proc. SPIE*, 1990, **1306**, 69–80.

20 **Hall, D. L.** and **Llinas, J.** An introduction to multisensor data fusion. *Proc. IEEE*, 1997, **85**(1), 6–23.

21 **Wang, P.** *Fuzzy sets and their applications*, 1983 (Shanghai Science and Technology Press, Shanghai).

22 **Zadeh, L. A.** Fuzzy sets. *Inf. Control*, 1965, **8**, 338–353.